Magnetic Circular Dichroism Study of Cytochrome ba_3 from *Thermus thermophilus*: Spectral Contributions from Cytochromes *b* and a_3 and Nanosecond Spectroscopy of CO Photodissociation Intermediates†

Robert A. Goldbeck,*,‡ Ólöf Einarsdóttir,‡ Timothy D. Dawes,‡ Donald B. O'Connor,‡ Kristene K. Surerus,§ James. A. Fee,§ and David S. Kliger*,‡

Department of Chemistry and Biochemistry, University of California at Santa Cruz, Santa Cruz, California 95064, and Biochemistry Section and Stable Isotope Resource, Division of Isotope and Nuclear Chemistry, Mail Stop C-345, Los Alamos National Laboratory, Los Alamos, New Mexico 87545

Received December 24, 1991; Revised Manuscript Received June 17, 1992

ABSTRACT: Near-UV–vis magnetic and natural circular dichroism (MCD and CD) spectra of oxidized, reduced, and carbonmonoxy-complexed cytochrome ba_3, a terminal oxidase from the bacterium *Thermus thermophilus*, and nanosecond time-resolved MCD (TRMCD) and CD (TRCD) spectra of the unligated species formed after photodissociation of the CO complex are presented. The spectral contributions of individual cytochromes *b* and a_3 to the Soret region MCD are identified. TRMCD spectroscopy is used to follow the spin state change ($S = 0$ to $S = 2$) in cytochrome a_3^{2+} following photodissociation of the CO complex. There is prompt appearance of the high-spin state after photolysis, as found previously in mammalian cytochrome oxidase [Goldbeck, R. A., Dawes, T. D., Einarsdóttir, Ó., Woodruff, W. H., & Kliger, D. S. (1991) *Biophys. J. 60*, 125–134]. Peak shifts of 1–10 nm appear in the TRMCD, TRCD, and time-resolved UV–vis absorption spectra of the photolyzed enzyme throughout its observable lifetime, indicating that the photolyzed enzyme does not relax to its equilibrium deliganded form before recombination with CO occurs hundreds of milliseconds later. Direct heme–heme interaction is not found in cytochrome ba_3, but red-shifts in the MCD and absorption spectra of both cytochromes *b* and (photolyzed) a_3 are correlated with a CO-liganded form of the protein. The long time ($\tau \gtrsim 1$ s) needed for relaxation of the cytochrome *b* and a_3 peaks to their static positions suggests that CO binding to a_3 induces a global conformational change in the protein that weakly perturbs the MCD and absorption spectra of *b* and photolyzed a_3. Fe_{a_3} binds CO more weakly in cytochrome ba_3 than in cytochrome aa_3. The MCD spectrum of reduced enzyme solution placed under 1 atm of CO contains a peak at 446 nm that shows ~30% of total cytochrome a_3 remains pentacoordinate, high-spin.

Heme- and copper-containing proteins serve as terminal oxidases of aerobic respiratory systems. Cytochromes designated aa_3, caa_3, *cao*, *bo*, *ba*, and ba_3 constitute a family of enzymes that transfer electrons from either cytochromes *c* or quinols to O_2 in a process that involves translocation of protons across a membrane (Anraku, 1988; Chepuri et al., 1990; Mather et al., 1990; Saraste et al., 1990). The phenomenon of redox-linked proton pumping is one of nature's elementary motifs for energy transduction. While not experimentally established for all the heme–Cu oxidases, proton pumping is likely to be a general property of these proteins, and understanding its mechanism remains an important goal of workers in the field.

Eukaryotic cytochrome aa_3 has been studied for nearly a century and is the characteristic member of the heme–copper oxidase family [cf. Wikström et al. (1985)]. Depending on the source, the isolated protein contains from 7 to 13 different protein subunits and two hemes A (formyl heme) and two copper atoms in unique functional sites, as well as additional Cu (Cu_x), Zn, and Mg (Einarsdóttir & Caughey, 1985; Pan et al., 1991) whose functions remain elusive. During the past decade, work with bacterial enzymes having only one to three subunits has led to the recognition that these enzymes are homologs of the eukaryotic enzyme. The emerging picture is that subunits I, II, and III, encoded by mitochondrial genes, constitute the core of the eukaryotic enzyme and that homologs of these subunits compose the bacterial heme–Cu oxidases. The cytochrome caa_3 from *Thermus thermophilus*, in particular, has been widely characterized by physical methods confirming the essential identity of the metal-binding sites in prokaryotic and eukaryotic enzymes [cf. Fee et al. (1986)]. More recently, molecular genetic approaches have established amino acid sequence homology of the *Thermus* subunits (I, IIc, and III) to all other aa_3-type cytochromes (Fee et al., 1988; Mather et al., 1991).

The four canonical metals are bound in distinctly different coordination environments. One of the hemes, designated cytochrome *a* (heme A) or cytochrome *b* (heme B, protoheme), appears to be axially coordinated to two histidine residues; it remains low-spin in both Fe^{2+} and Fe^{3+} valence states and is magnetically isolated from the other metal centers. One of the Cu ions, Cu_A, appears to be coordinated to two histidine residues and two cysteine thiolates and is magnetically isolated from the other metal centers. (Cu_A is not present in all the heme–Cu oxidases.) The second heme, comprising cytochrome a_3 (heme A) or cytochrome *o* [heme B, cf. Puustinen and Wikström (1991)], appears to be axially coordinated to one histidine and has an open axial coordination position. Optical spectra of the oxidized protein suggest that the Fe^{3+} form of cytochrome a_3 is high-spin ($S = {}^5/_2$), while EPR and

† This work was financially supported in part by the National Institutes of Health, Grants GM-38549 (D.S.K.) and GM-35342 (J.A.F.). K.K.S. was the recipient of a Director's Fellowship from Los Alamos National Laboratory.

‡ University of California at Santa Cruz.

§ Los Alamos National Laboratory.

0006-2960/92/0431-9376$03.00/0

magnetic susceptibility studies have revealed that this heme is in very close proximity to the second Cu, Cu_B. In the oxidized form of the protein, the electronic spins of these two metals interact in a yet unknown manner to render both metals EPR silent. Cu_B has no strong absorptions in the UV–vis region and is presumably bound to four histidine residues. In the reduced form of the enzyme, $a_3(o)$–Fe^{2+} is five-coordinate and high-spin ($S = 2$). The cytochrome $a_3(o)$–Cu_B cluster is the site of dioxygen reduction [cf. Chan and Li (1990)].

Cytochrome ba_3, the subject of this paper, is the second terminal oxidase isolated from the plasma membrane of *T. thermophilus* and was originally described as a single subunit, ~35-kDa protein similar to cytochrome aa_3 (Zimmerman et al., 1988). Recent results from molecular genetic studies of this enzyme[1] show a gene structure for cytochrome ba_3 that is very similar to that of the *Thermus* cytochrome caa_3 (Fee et al., 1988), suggesting that additional protein subunits may be present in this protein. Nevertheless, the four redox-active metal sites present in cytochrome aa_3, two copper ions (Cu_A and Cu_B) and two hemes (cytochromes *a* and a_3), are also present in cytochrome ba_3, with the major difference being the replacement of heme A with heme B at the cytochrome *a* site; thus, cytochrome ba_3 (Zimmerman et al., 1988).

The $a_3(o)$–Fe^{2+} site of the heme–copper oxidases is able to bind a single carbon monoxide molecule that photodissociates from a_3^{2+} with high quantum yield and transfers to Cu_B^{1+} (Fiamingo et al., 1982; Einarsdóttir et al., 1989). The CO complex of eukaryotic oxidases has been used extensively in time-resolved spectral studies as a model for O_2 binding and as a photolytic source of unliganded enzyme for reaction with dissolved oxygen. However, the results of several recent studies reveal that photodissociation of the CO complex is a more complicated event than previously believed. An IR study of cytochrome ba_3–CO showed that photodissociation of the Fe–CO bond leads to quantitative binding of CO with Cu_B (Einarsdóttir et al., 1989). Time-resolved IR studies of cytochrome aa_3–CO photolysis at room temperature have directly observed binding of CO to Cu_B after photolysis (Dyer et al., 1991) and later decay of the Cu–CO complex with a 1.5-μs half-life (Dyer et al., 1989). The possibility that Cu_B may sequester small exogenous ligands such as CO as they leave and enter the heme pocket has important consequences for models of O_2 binding and for the interpretation of flow-flash:O_2-reduction studies with these enzymes (Chance et al., 1975; Babcock et al., 1984; Blackmore et al., 1991). Furthermore, time-resolved resonance Raman (TR^3) and UV–vis absorption (TROD) studies of the mammalian oxidase have led Woodruff and co-workers to suggest that an endogenous, photolabile ligand shuttles between coordination to cytochrome a_3–Fe^{2+} and to Cu_B^+ (Woodruff et al., 1991). This unexpected complexity in the mechanism of CO photodissociation and rebinding in bovine cytochrome *c* oxidase has prompted studies of CO photolysis using a recently developed technique for nanosecond time-resolved magnetic circular dichroism (TRMCD) spectroscopy (Goldbeck et al., 1989, 1991; Kliger et al., 1989; Dawes, 1990).

The MCD of cytochrome oxidase is sensitive to the spin and oxidation state of the two heme chromophores (Babcock et al., 1976; Carter & Palmer, 1982). This sensitivity is exploited in TRMCD studies to monitor coordination changes at cytochrome a_3 during photodissociation and rebinding of ligand complexes. The binding of small ligands, such as CO, to cytochrome a_3–Fe^{2+} changes the spin state of ferrous heme from high- ($S = 2$) to low-spin ($S = 0$). The loss of spin degeneracy accompanying ligand binding is signaled in the MCD spectrum by a large decrease in magnitude in the Soret region (the 400–450-nm region containing intense absorption bands characteristic of porphyrins) caused by disappearance of intense, paramagnetic C terms associated with high-spin ferrous heme (Babcock et al., 1976; Carter & Palmer, 1982). Because the second heme chromophore contributing to the MCD of cytochrome ba_3 (aa_3), cytochrome *b* (*a*), is always six-coordinate low-spin, it is expected to provide a nearly constant background to the large MCD changes observed for cytochrome a_3 when a_3–Fe^{2+} gains or loses a sixth ligand. However, ligation changes at heme a_3 could affect the MCD of the second heme by inducing small structural changes, and the extent to which this occurs in cytochrome ba_3 is examined in the present study.

The correlation of spin state with axial ligation of the cytochrome a_3–Fe^{2+} allows TRMCD spectroscopy to be used as a time-resolved probe of a_3 coordination. The information available from TRMCD complements information from other time-resolved spectroscopies. In a previous TRMCD study of bovine cytochrome *c* oxidase (Goldbeck et al., 1989) we found that the photolyzed complex went to a high-spin state within the nanosecond time resolution of our instrument and stayed high-spin until CO recombination occurred milliseconds later, implying that a_3–Fe^{2+} remains five coordinate after CO photolysis. However, failure to detect the Fe–imidazole stretching band in TR^3 measurements suggested either that Fe remains six coordinate 100 ns after photolysis or that coordination of Fe to the proximal histidine is lost (Woodruff et al., 1991); the latter interpretation of the TR^3 results is consistent with the TRMCD evidence. The present body of time-resolved spectral evidence for cytochrome aa_3 has been interpreted in terms of a model of CO photodissociation that involves binding of an endogenous ligand to the distal side of the iron and concomitant loss of imidazole coordination at the proximal site (Woodruff et al., 1991).

In this report we present the MCD and CD spectra of *T. thermophilus* cytochrome ba_3 and TRMCD and TRCD evidence characterizing the deliganded species formed after photodissociation of the CO complex. Ferrous cytochrome *b* has a much smaller MCD intensity in the Soret region than does ferrous cytochrome *a* (of aa_3), allowing a clearer view in cytochrome ba_3 of spin state changes in the TRMCD spectrum of cytochrome a_3 than in cytochrome aa_3. A high-spin state appears promptly in cytochrome a_3 after photodissociation of CO from cytochrome ba_3, as found previously for CO photolysis in eukaryotic oxidase. The TRMCD, TRCD, and time-resolved UV–vis absorption spectra show that the photolyzed enzyme does not relax to the equilibrium, unliganded form of the protein within the Fe–CO recombination lifetime (0.1 s). An examination of the MCD and CD spectral properties of the two heme centers in cytochrome ba_3 finds no direct electronic heme–heme interaction but suggests that protein structural changes resulting from CO ligation at the heme A site are transmitted to the heme B binding site.

MATERIALS AND METHODS

Details of the preparation of cytochrome ba_3 samples from *T. thermophilus* have been presented elsewhere (Zimmerman et al., 1988; Zimmerman, 1989). The enzyme was fully reduced using sodium dithionite under nitrogen or argon atmosphere. The CO complex was prepared by flowing CO gas at 1 atm pressure over reduced enzyme solution. All spectra were obtained using 5–8 μM solutions, on a mole of

[1] J. A. Keightley and J. A. Fee, unpublished results.

heme a_3 per liter basis and were smoothed using a 25 point (0.6 nm/point) Savitzky-Golay (1964) smoothing algorithm. All extinction coefficients are reported on a per molar heme A basis.

Equilibrium and time-resolved CD and MCD spectra were measured using an ellipsometric method that has been described in detail elsewhere (Goldbeck et al., 1989, 1991; Kliger et al., 1989, 1990; Dawes, 1990). Briefly, the technique employs a nanosecond laser-photolysis apparatus modified by the addition of polarization controlling optics to measure changes (caused by the CD, MCD of the sample) in the eccentricity of an elliptically polarized probe beam. TRMCD measurements employed a 0.64-T permanent magnet (JASCO PM-2) and a polarization rotator (sucrose or fructose solution) to compensate for Faraday rotation of the probe polarization ellipse by the magnetic field. The sample was photolyzed with a 532-nm, 20-mJ, 7-ns pulse from a frequency-doubled Nd:YAG laser (Quanta-Ray DCR-11), giving a photolysis yield of 80%. (As discussed below, all time-resolved spectra of transient species have been corrected to 100% yield.) The probe source was a 5-μs duration xenon flashlamp (EG&G FX-193) operated at 4 J of electrical energy per flash. Time-resolved spectra were obtained by detecting the probe beam with an optical multichannel analyzer (OMA) instrument that consists of a spectrograph (Jarrell-Ash Monospec 27, 250-μm slit, 150 g/mm), gated detector (EG&G 1420), and detector interface (EG&G 1461).

Correction of Spectra for Incomplete Complex Formation and Photodissociation Yield. The correction of absorption spectra is considered first. The following notation is used to (1) distinguish observed spectra from spectra corrected for incomplete complex formation and photodissociation yield and (2) distinguish the spectrum of equilibrium reduced cytochrome ba_3 from the spectra of enzyme formed by photodissociation and thermal dissociation of the a_3–CO complex, as these may correspond to different conformations of the protein: ϕ, Fe_{a_3}–CO photodissociation yield; f, mole fraction of Fe_{a_3}–CO complex in equilibrium with nonligated Fe_{a_3}; OC(λ), observed spectrum of cytochrome ba_3–CO, uncorrected for non-CO ligated Fe_{a_3}; ODP(λ), observed difference spectrum of photolyzed CO complex; C(λ), spectrum of fully formed complex; DP(λ), difference spectrum of photolyzed complex, corrected for ϕ and f; U(λ), spectrum of equilibrium unliganded, reduced cytochrome ba_3; U*(λ), spectrum of photodissociated complex (conformationally unrelaxed); U‡(λ), spectrum of thermally dissociated complex (conformationally unrelaxed). The observed spectrum of the complex, OC, is a composite of the absolute spectrum of the complex, C, and thermally dissociated complex, U‡:

$$OC = fC + (1-f)U^\ddagger \tag{1}$$

The observed photolysis difference spectrum is given by

$$ODP = f\phi U^* + f(1-\phi)C + (1-f)U^\ddagger - OC$$

$$= f\phi(U^* - C) \tag{2}$$

The corrected photolysis spectrum, DP = U* – C, is obtained from the observed spectrum by

$$DP = ODP/(f\phi) \tag{3}$$

From eqs 1 and 2, it can be shown that

$$U^* = [ODP/\phi + OC - (1-f)U^\ddagger]/f \tag{4}$$

If U* and U‡ are indistinguishable, i.e., deliganded spectra measured before relaxation of the CO-liganded protein conformation are identical whether formed by photodissociation or thermal dissociation, then both can be represented by the symbol U†:

$$U^* \approx U^\ddagger \equiv U^\dagger \tag{5}$$

Then eq 4 simplies to

$$U^\dagger = ODP/\phi + OC \tag{6}$$

This relation for U†, combined with eq 1, leads to the following expression for the corrected spectrum of the complex in terms of observed spectra:

$$C = OC - ODP(1-f)/(f\phi) \tag{7}$$

In order to correct CD and MCD spectra for incomplete photolysis and complex formation, the symbols defined above for absorption spectra are carried over, and the following new quantity is defined

$$OP(\lambda) = \text{observed absolute spectrum of photolyzed CO complex}$$

The observed spectrum of photolyzed complex is related to other quantities by

$$OP = f\phi U^* + f(1-\phi)C + (1-f)U^\ddagger \tag{8}$$

If the approximation used in eq 5 is used again in eq 8, it can be shown that the corrected photolysis MCD (CD) spectrum is given by

$$U^\dagger = [OP - (1-\phi)OC]/\phi \tag{9}$$

and the corrected spectrum of the complex is given by

$$C = OC - (OP - OC)(1-f)/(f\phi) \tag{10}$$

The mole fraction, f, of complex present in the carbon monoxide–enzyme preparation is estimated under Results from the Soret region MCD signal arising from non-CO ligated cytochrome a_3. The quantity $1-f$ is determined from the ratio of the Soret maxima of non-CO ligated a_3 present in the CO–enzyme preparation and unliganded reduced enzyme. The photolysis yield, ϕ, is estimated from the observed absorption spectra, U, OC, and ODP. The observed differential absorption between equilibrium unliganded enzyme and the CO–enzyme preparation is defined as ΔA = U – OC. The bandshapes of ΔA and ODP are very similar near their band maxima in the Soret, allowing ϕ to be determined from their ratio. In the approximation that U* $\approx$ U‡ $\approx$ U, $\Delta A \approx f$(U – C) and ODP $\approx f\phi$(U – C), which leads to the relation

$$\phi = ODP(\lambda)/\Delta A(\lambda) \tag{11}$$

Soret band maxima of ODP(λ) and $\Delta A(\lambda)$ near 445 nm were used to estimate ϕ from eq 11. A more exact expression for ϕ is provided by

$$\phi = \frac{ODP}{\Delta A}\left(1 + \frac{U - U^\dagger}{\Delta A}\right)^{-1} \tag{12}$$

The quantity $(U - U^\dagger)/\Delta A$ was found to be less than 0.05 at 445 nm for cytochrome ba_3, confirming the validity of eq 11.

RESULTS

MCD of Oxidized Enzyme. The MCD spectrum of oxidized cytochrome ba_3 is shown in Figure 1(dashed line) and summarized in Table I. The Soret MCD has a roughly symmetric, derivative shape with negative lobe at low energy and zero-crossing slightly blue-shifted from the 416 nm absorption maximum. The spectrum is generally similar in

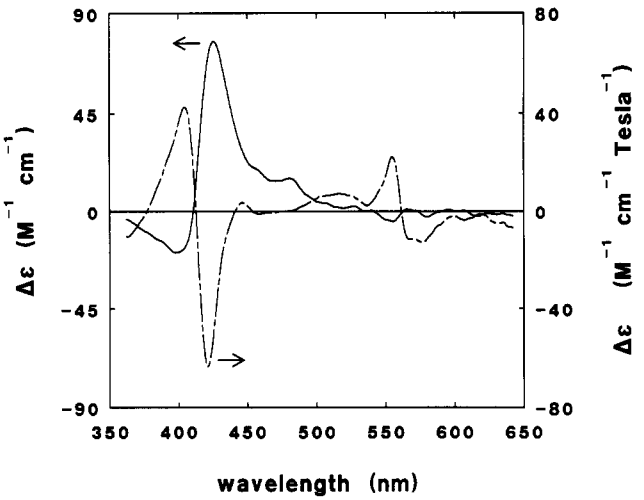

FIGURE 1: CD (—) and MCD (- - -) spectra of fully oxidized cytochrome ba_3. Note that CD and MCD are plotted on different intensity scales.

Table I: MCD Spectral Characteristics of *T. thermophilus* Cytochrome ba_3

species	band extrema (nm)	Δε/H (M^{-1} cm^{-1} T^{-1})	species	band extrema (nm)	Δε/H (M^{-1} cm^{-1} T^{-1})
oxidized	405	42	photolyzed, 100 ns[b]	~425	-35
	421	-63		446	122
	447	4		513	20
	517	7		537	-9
	555	22		556	110
	577	-13		565	-123
reduced	432	-35	photolyzed, 10 μs[b]	~425	-35
	445	117		446	122
	513	20		513	20
	536	-14		536	-14
	556	120		556	110
	564	-134		565	-123
reduced + CO[a]	420	-7			
	429	3			
	435	-6			
	446	36			
	513	20			
	537	-9			
	556	110			
	565	123			

[a] Uncorrected for Fe–CO binding. [b] Corrected to 100% photolysis.

both the Soret and visible bands to the spectrum of cytochrome b_5^{3+} (Vickery et al., 1976). This is consistent with the expectation from the eukaryotic enzyme (Babcock et al., 1976) that the Soret MCD of cytochrome a_3^{3+} is quite weak, leaving cytochrome b^{3+} as the dominant contributor to the spectrum of the bacterial enzyme. The similarity to the well-characterized MCD spectrum of cytochrome b_5 supports the assignment of bis(histidine) ligation for the heme B center in cytochrome ba_3.

The low-energy visible region shows derivative type MCD with a zero-crossing at 562 nm, similar to the *A* term associated with the Q_0 bands of ferricytochrome b_5. The intensity of the positive lobe at 555 nm is about double that seen in ferricytochrome b_5, while the negative lobe has a peculiar shape with double humps at 568 and 577 nm. The 568-nm peak corresponds closely in intensity and wavelength with the negative lobe at 570 nm in ferricytochrome b_5, which suggests that the longer wavelength peak is due to cytochrome a_3^{3+}. However, it is not clear how much of the spectral difference observed between the Q_0 bands in ferricytochromes ba_3 and b_5 can be attributed to cytochrome a_3^{3+} and how much is due

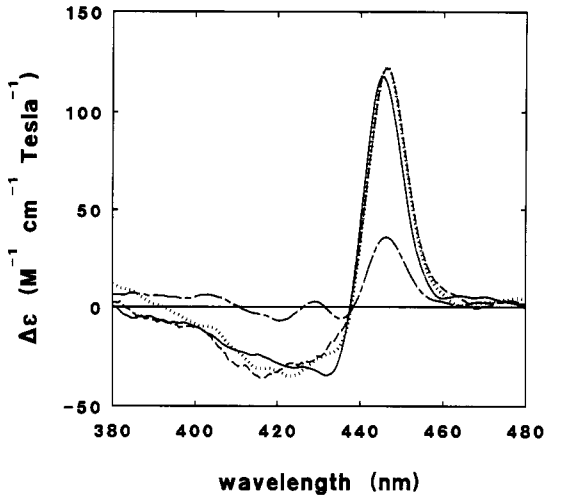

FIGURE 2: Soret region MCD of equilibrium reduced cytochrome ba_3 (—) and the CO complex (- - -), and the TRMCD of cytochrome ba_3–CO at 100–300 ns (- - -) and 10–12 μs (···) after CO photodissociation. The TRMCD is corrected to 100% photolysis. The TRMCD and CO complex spectra are of the 1 atm CO–enzyme preparation without correction for incomplete formation of Fe_{a_3}–CO (see text).

to the differing protein environments of the heme B chromophores in cytochrome b_5 and cytochrome *b*.

The general similarity between the near-UV–vis MCD spectra of oxidized ba_3 and b_5 includes the small positive peak present near 517 nm in both species, although a small positive peak seen near 480 nm in b_5 is not present in ba_3. The MCD activity of ferricytochromes in the spectral region near 480 nm has been assigned to *C* terms associated with charge-transfer transitions and tends to be very ligand dependent (Vickery et al., 1976). The Soret region MCD of resting ba_3 is also similar in bandshape and sign to aa_3 (Babcock et al., 1976), although it is blue-shifted and more intense than aa_3. In the α band region (Q_0 band), on the other hand, the MCD spectra of ferricytochromes b_5 and ba_3 are qualitatively different from the spectrum of aa_3. The latter has an *A* term centered at 596 nm that is opposite in sign and considerably less intense than that found in the cytochrome *b* species. This divergence in sign for the α band MCD is probably caused by the difference in peripheral substituents on the porphyrin ring in heme A and heme B, a point that is discussed further below in connection with the Soret band MCD intensities.

MCD of Reduced Enzyme and CO Complex. The Soret region spectrum of the reduced enzyme shown in Figure 2 is the sum of an intense, paramagnetic deoxyhemoglobin-like spectrum contributed by cytochrome a_3^{2+} and a weaker (by a factor of 10), diamagnetic ferrocytochrome-like spectrum from cytochrome b^{2+}. The a_3 component has a positive extremum near 445 nm, close to the a_3 absorption maximum, and a smaller negative extremum at 432 nm. The negative lobe of the a_3 contribution obscures the cytochrome *b* contribution, which is expected to lie near the *b* absorption maximum ca. 427 nm. The CO complex, in contrast to the unliganded enzyme, is also expected to have weak (more than an order of magnitude smaller than the high-spin cas) MCD in the Soret region. Babcock et al. (1976) found that the Soret MCD contribution of low-spin cytochrome a_3^{2+} is nearly negligible in cytochrome aa_3. The contribution from cytochrome b^{2+} is expected from the reported MCD spectrum of cytochrome b_5^{2+} (Vickery et al., 1975; Dolinger et al., 1974) to have more intensity than the low-spin a_3^{2+} contribution and much less intensity than high-spin a_3^{2+}. On this basis, it is clear that the large, positive MCD extremum seen at 446

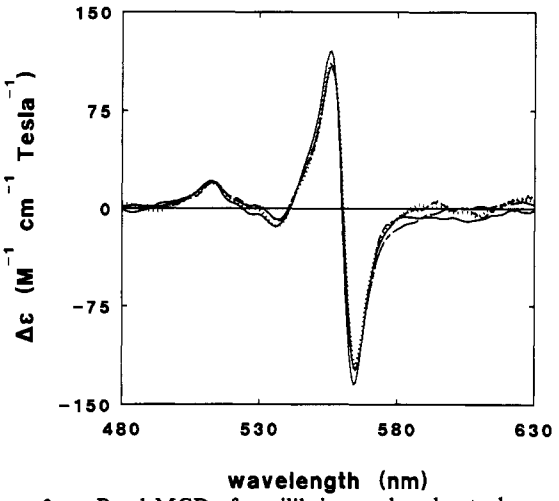

FIGURE 3: α-Band MCD of equilibrium reduced cytochrome ba_3 (—) and the CO complex (- - -), and the TRMCD of cytochrome ba_3–CO at 100–300 ns (- - -) and 10–12 μs (···) after CO photodissociation, uncorrected for Fe_{a_3}–CO binding (see Figure 2 legend).

nm in Figure 2 for the CO–enzyme preparation arises from neither cytochrome a_3–CO nor cytochrome b^{2+} but must be due to the presence of high-spin cytochrome $a_3{}^{2+}$. The presence of high-spin heme a_3 in these samples indicates that formation of the heme a_3–CO complex does not go to completion under these conditions. This identification is strengthened by the identical bandshapes of the 446-nm band in the CO preparation and the 445-nm band in the reduced enzyme preparation, after adjustment for the spectral shift and intensity difference. We conclude from the ratio of MCD intensities in Table I that 30% of cytochrome a_3 remains high-spin, non-CO-ligated in cytochrome ba_3 under 1 atm of CO, and, as discussed further below, we infer from the presence of the spectral shift that this fraction is in equilibrium with the complex.

The visible region MCD spectra of reduced cytochrome ba_3 and the CO complex (Figure 3) are dominated by the intense *A* term, associated with the Q_0 band of cytochrome b^{2+} (561 nm in the absorption spectrum), which is typical of diamagnetic metalloporphyrins. Therefore, only small spectral differences are evident between the liganded, unliganded, and photolyzed ba_3 species. There is a slightly larger peak to trough intensity and small blue-shift (0.4 nm) of the Q_0 MCD band of unliganded cytochrome ba_3 compared with the CO-complexed and photolyzed enzyme. A second, weaker *A* term or quasi-*A* term with zero crossing near 530 nm is assigned to the Q_1 band (529-nm absorption maximum) of cytochrome b^{2+}. The only evidence of MCD activity for cytochrome $a_3{}^{2+}$ seen in the visible region is the small shoulder near 580 nm in the spectrum of the CO complex. In mammalian cytochrome oxidase, a similar increase in magnitude of a negative MCD peak at 580 nm is also associated with formation of the CO complex (Goldbeck et al., 1991).

Soret CD Spectra. The Soret region CD spectrum of resting cytochrome ba_3, shown in Figure 1 (solid line), has a positive lobe at 426 nm and a weaker negative lobe at 398 nm (Table II) with a zero-crossing at 411 nm that is blue-shifted from the Soret absorption band maximum at 416 nm. The spectrum of the reduced protein (positive peak at 439 nm, Figure 4) is red-shifted and more intense than the oxidized spectrum. The negative trough nearly triples in depth with reduction, giving a bandshape more similar to the derivative of the absorption spectrum. Formation of the CO complex blue-shifts the positive CD lobe by 3 nm and decreases its intensity while increasing the intensity of the negative lobe (Figure 4).

Table II: CD Spectral Characteristics of *T. thermophilus* Cytochrome ba_3

species	band extrema (nm)	Δε (M^{-1} cm^{-1})	species	band extrema (nm)	Δε (M^{-1} cm^{-1})
oxidized	398	−19	reduced + CO[a]	420	−75
	426	77		436	95
	481	15		580	15
	555	−5	photolyzed, 100 ns[b]	421	−53
	580	−3		440	121
reduced	419	−52		577	8
	439	100	photolyzed, 10 μs[b]	420	−52
	555	−7		441	114
	572	7		577	8

[a] Uncorrected for Fe–CO binding. [b] Uncorrected to 100% photolysis.

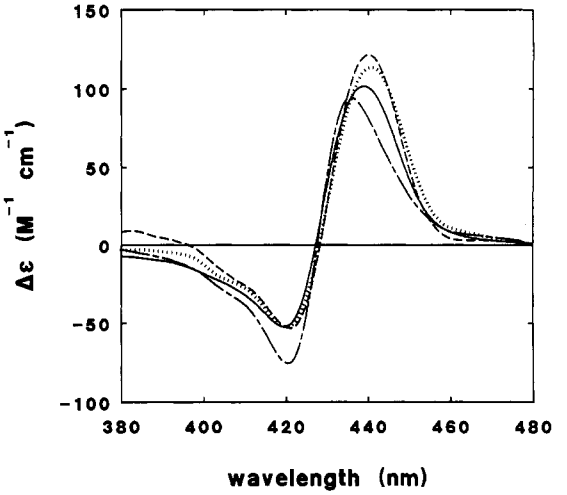

FIGURE 4: Soret region CD of equilibrium reduced cytochrome ba_3 (—) and the CO complex (- - -), and the TRCD of cytochrome ba_3–CO at 100–300 ns (- - -) and 10–12 μs (···) after CO photodissociation, uncorrected for Fe_{a_3}–CO binding (see Figure 2 legend).

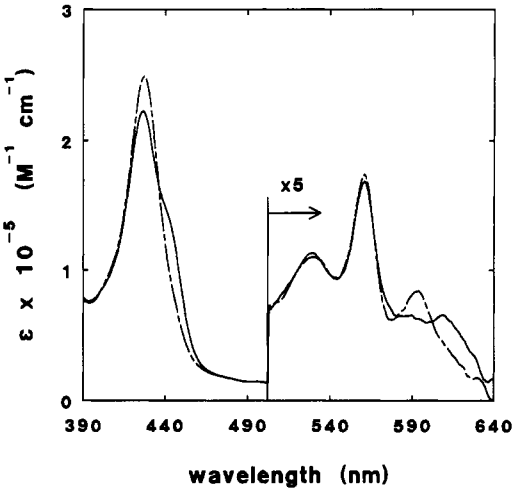

FIGURE 5: Absorption spectra of fully reduced cytochrome ba_3 (—) and the CO complex (- - -). The latter is the spectrum of the 1 atm CO–enzyme preparation, uncorrected for incomplete formation of Fe_{a_3}–CO (see text).

Absorption Spectra of Reduced Enzyme and CO Complex. The absorption spectra of fully reduced cytochrome ba_3 and its CO complex (uncorrected for *f*) are presented in Figure 5. The absorption spectrum of unliganded ba_3 has a peak at 427 nm and a shoulder at 442 nm. The overlapping individual contributions of cytochromes *b* and a_3 to the Soret absorption spectrum of the reduced enzyme are more evident in the second-derivative spectrum shown in Figure 6. The absorption band

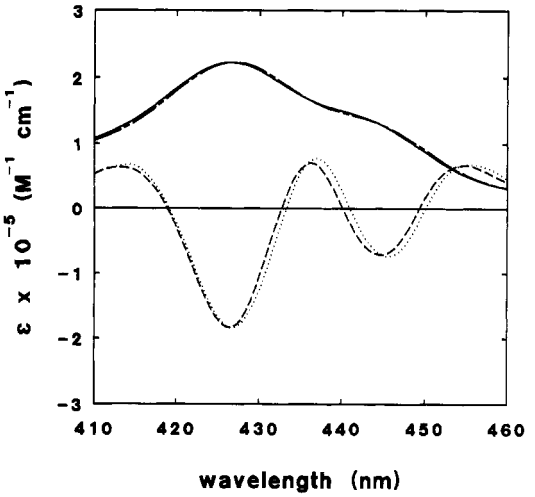

FIGURE 6: Observed Soret region absorption spectrum of reduced cytochrome ba_3 (U) (—), the calculated absorption spectrum of photolyzed enzyme (U* in text) (- - -), and the second-derivative spectra of U (- - -) and U* (···).

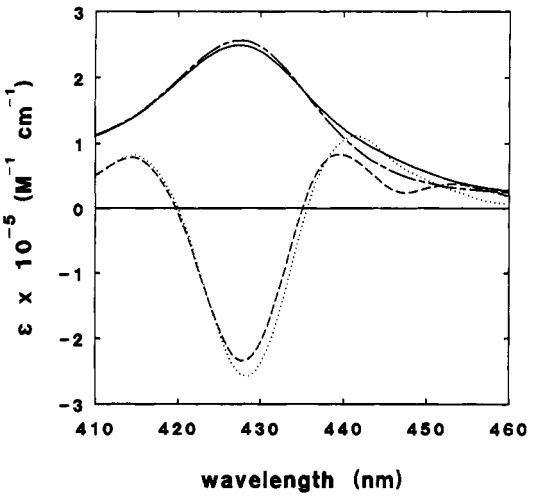

FIGURE 7: Observed Soret region absorption spectrum of cytochrome ba_3 + CO (—) and its second derivative (- - -). The calculated absorption spectrum of cytochrome ba_3–CO (– – –) corrected to full formation of the complex using equation 7 (f = 1) and its second derivative (···).

maxima of b and a_3 appear as second-derivative minima at 426 and 444 nm, respectively. (Difference or derivative spectra containing overlapping Gaussian-like components will not necessarily have extrema exactly in register with the absolute spectra of the components or their sum.)

As in mammalian enzyme, binding of CO to cytochrome ba_3 blue-shifts the Soret absorption of the cytochrome a_3 component. The absorption peak of the complex is red-shifted slightly to 428 nm and is higher in intensity than the peak of the unliganded enzyme. The individual bands for cytochromes b and a_3-CO overlap closely and are not resolved in the absolute or second-derivative spectra. However, the second-derivative spectrum, shown in Figure 7, does reveal the presence of an additional component underlying the red edge of the band, near 448 nm. This component corresponds to the non-heme-CO ligated fraction identified in the MCD spectrum. A spectrum for the CO complex without the unligated fraction, calculated using eq 7, is shown in Figure 7. The corrected spectrum has a slightly narrower bandshape and no second-derivative minimum at the red edge of the band.

The difference spectrum between the CO-liganded and unliganded forms of the bacterial enzyme, shown in Figure

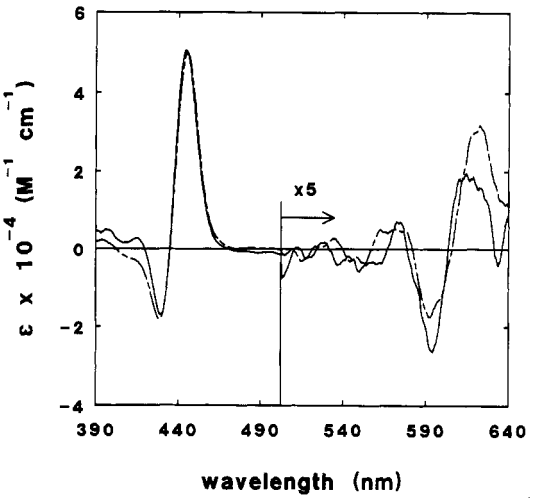

FIGURE 8: Absorption difference spectrum between reduced cytochrome ba_3 at equilibrium and its CO complex (—) and the time-resolved absorption difference between the photolyzed and unphotolyzed CO complex (- - -) taken at 10 μs after photolysis (corrected to 100% photolysis). Spectra were not corrected for incomplete complex formation (see text).

8, is smaller and less symmetric in the Soret region than the difference spectrum of mammalian oxidase. This suggests that the heme a_3–CO Soret bandshape is broadened and red-shifted in the bacterial enzyme. However, some of the diminished difference intensity is attributable to incomplete formation of the Fe_{a_3}–CO complex in the bacterial enzyme ($f < 1$), as discussed below.

The visible-region spectrum of the reduced enzyme in Figure 5 has peaks at 562 and 613 nm typical of b and a type cytochromes. These are assigned to cytochromes b and a_3, respectively (Zimmerman et al., 1988). As expected from this assignment, CO binding strongly blue-shifts the 613-nm peak and leaves the 562-nm peak unshifted. The small difference in intensity at 562 nm between liganded and unliganded enzyme is probably caused by a change in the vibronic (Q_1) contribution of a_3 underlying the b absorption band. In contrast to the Soret region difference spectrum, the visible difference spectrum of cytochrome ba_3 shows a greater shift of the a_3 peak with CO binding than is found in cytochrome aa_3. The visible and Soret absorption bands of the complex do not show obvious evidence for spectral perturbation of cytochrome b by CO binding at cytochrome a_3.

Time-Resolved Absorption Spectra of CO Photodissociation. The difference spectrum (unliganded CO complex) of reduced ba_3 species at equilibrium and the time-resolved difference spectrum after photodissociation (CO complex + $h\nu$ – CO complex), corrected to 100% yield from the observed 80% photolysis yield, are shown in Figure 8. (These spectra are not adjusted for incomplete complex formation.) They are similar but not identical in the Soret region (peaks ca. 445 nm, troughs ca. 429 nm). There is a small (<1 nm) red-shift of the Soret peak of the photolysis spectrum compared with the equilibrium difference spectrum. Differences are more evident in the visible region: the red-shift of the 623-nm peak in the photolysis spectrum from the corresponding peak at 611 nm in the equilibrium difference spectrum provides a clearer indication that the photolyzed enzyme has not completely relaxed after 10 μs.

Time-Resolved MCD. The TRMCD spectrum of photolyzed complex is similar to the MCD of the steady-state, unliganded enzyme (Figure 2), reflecting the electronic state change of the ferrocytochrome a_3 heme iron from low

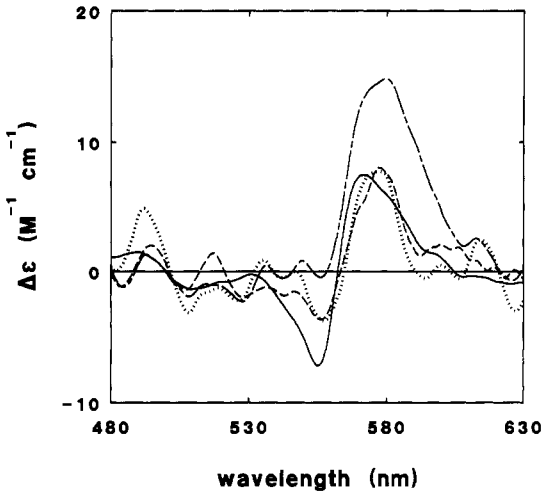

FIGURE 9: α-Band CD of equilibrium reduced cytochrome ba_3 (—) and the CO complex (– – –), and the TRCD of cytochrome ba_3–CO at 100–300 ns (- - -) and 10–12 μs (•••) after CO photodissociation, uncorrected for Fe_{a_3}–CO binding (see Figure 2 legend).

(diamagnetic) to high (paramagnetic) spin as the sixth ligand is photodissociated from the heme. The location of the TRMCD peak (446 nm) for both the 100-ns and 10-μs transient spectra (Table I) is slightly red-shifted from the Soret peak of the equilibrium unliganded MCD spectrum, indicating that the environment around heme A remains unrelaxed after 10 μs. The unrelaxed character of the photolyzed enzyme is also evident in the smaller peak to trough intensity and red-shift of the Q_0 MCD band compared with the equilibrium enzyme.

Time-Resolved CD. Photodissociation of CO produces photolyzed enzyme with a Soret CD similar to equilibrium unliganded protein, as Figure 4 shows. However, the red-shift of the positive CD lobe and its increased intensity in the photolyzed enzyme compared with the steady-state, deliganded CD is another indication of the unrelaxed character of the protein structure surrounding cytochrome a_3 after photolysis. The visible band CD spectra in Figure 9 also suggest that the photolyzed has a heme A electronic structure similar to the unliganded enzyme but perturbed from the steady-state structure by the unrelaxed conformation of the protein. The pattern of intensities in the photolyzed CD spectra is qualitatively similar to that in the unliganded enzyme, but the positive CD peak of the photolyzed enzyme (Table II) near 577 nm is closest in energy to the peak at 580 nm for the equilibrium CO-liganded enzyme.

DISCUSSION

Electronic States of Heme A and Heme B in the Oxidized Enzyme. Mitochondrial cytochrome a_3^{3+} is known to be high-spin ($S = {}^5/_2$) and possess very weak MCD in the Soret region (Babcock et al., 1976). EPR spectroscopy of oxidized cytochrome ba_3 shows the presence of a low-spin heme B (Zimmerman et al., 1988). Mössbauer spectroscopy of ba_3 shows that heme A is high-spin and magnetically coupled to $Cu_B^{2}1+$ ($S = {}^1/_2$) to yield an EPR silent even-spin system (Zimmerman et al., 1988). Hence, the results of previous MCD studies of resting cytochrome aa_3 and EPR and Mössbauer studies of resting cytochrome ba_3 support the assignment here of the MCD band centered at 413 nm in cytochrome ba_3 to low-spin ($S = {}^1/_2$), bis(histidine) ligated cytochrome b^{3+}. This derivative-shaped band has an inverse temperature dependence in oxidized cytochrome aa_3 and other low-spin ferric hemeproteins and has been assigned to a pair of oppositely signed C terms. The band intensity is proportional to the percentage of low-spin content for a wide variety of ligand complexes of ferric hemes with imidazole as the fifth ligand (Vickery et al., 1976) (a notable exception being complexes with thiolate ligands). The intensity of the band assigned here to cytochrome b^{3+} is typical of a 100% low-spin ferric hemeprotein. As noted above, this is significantly greater than the intensity deduced by Babcock et al. (1976) for cytochrome a^{3+} in resting cytochrome aa_3. The intensity of the MCD trough in the latter is roughly half that typical of ferric low-spin heme proteins (Dawson & Dooley, 1989). The difference in Soret intensity between cytochromes ba_3 and aa_3, which apparently have identical heme axial ligation, is probably due to the absence in heme B of the formyl and farnesylethyl substituents present in heme A. In particular, the strong π-electron withdrawing effect of formyl as a β-pyrrole substituent perturbs the electronic structure of the porphyrin ring in a manner that can invert the sign of the low-lying electronic MCD from that observed in unsubstituted porphyrins (Michl, 1978; Goldbeck, 1988). This effect is stronger in the visible bands than in the Soret (Djerassi et al., 1984), which accounts for the outright reversal of sign of the low-energy visible-band MCD spectrum of resting cytochrome aa_3 from that observed in ba_3.

Photodissociation of the CO Complex. The events following photolysis of the CO complexes of bacterial and eukaryotic cytochrome oxidase are qualitatively similar in that CO photodissociated from $Fe_{a_3}^{2+}$ binds to nearby Cu_B until it is released thermally. The residence time of CO on Cu_B is longer in the bacterial enzyme, allowing measurement of the absorption spectrm of the CO–Cu vibration using FTIR at ambient temperature (Einarsdóttir et al., 1989). Time-resolved IR measurements on eukaryotic oxidase, in contrast, found a short residence time (half-life of 1.5 μs) for CO on Cu_B (Dyer et al., 1989). CO released from eukaryotic Cu_B mainly diffuses from the protein at ambient temperature, since recombination with $Fe_{a_3}^{2+}$ requires milliseconds. Photodissociated CO that has diffused into solution must first recombine with Cu_B in a second-order rate process before it can reunite with cytochrome a_3. The two-step recombination reaction of reduced cytochrome a_3 with CO is shown below.

$$Fe_{a_3},Cu_B + CO_{(aq)} \underset{k_{-1}}{\overset{k_1}{\rightleftharpoons}} Fe_{a_3},OC\text{–}Cu_B \underset{k_{-2}}{\overset{k_2}{\rightleftharpoons}} Fe_{a_3}\text{–}CO,Cu_B$$

The first-order reaction rate k_2 for the transfer of CO from Cu_B to Fe_{a3} is faster in mammalian cytochrome aa_3 (700 s^{-1}) than in the bacterial oxidases caa_3 (60 s^{-1}) and ba_3 (8 s^{-1}).[2] The observed pseudo-first-order rate for return of Fe–CO optical absorption in cytochrome ba_3 is saturated at 11 s^{-1} for $CO_{(aq)}$ concentrations in the range 10^{-4}–10^{-3} M. This implies that establishment of the initial equilibrium $K_1 = k_1/k_{-1}$ is very rapid compared to formation of the final equilibrium $K_2 = k_2/k_{-2}$ and that Cu_B has a high affinity for CO. The values of k_2 and $k_2 + k_{-2}$ (observed k) imply that $K_2 \approx 3$ in cytochrome ba_3, a value that is consistent with the MCD findings for unliganded Fe_{a_3} in the CO-saturated enzyme.

Heme Spectral Shifts and Protein Relaxation. In order to examine more closely the issue of unrelaxed spectral characteristics for ferrous cytochromes b and a_3 after photodissociation of cytochrome ba_3–CO, it is useful to look at

[2] Ó. Einarsdóttir, P. M. Killough, J. A. Fee, and W. H. Woodruff, unpublished results. The CO recombination reaction of mitochondrial enzyme departs substantially from first-order kinetics at low temperatures, suggesting distributed activation enthalpy values (Fiamingo et al., 1982).

the absolute absorption spectrum of the photolyzed enzyme. This is calculated from the observed photolysis difference spectrum and the absorption spectrum of the CO–enzyme preparation using eq 6. (Equation 6 uses the approximation that the spectra of the uncomplexed component of the CO preparation and photolyzed enzyme are identical.) The result is shown in Figure 6. There is a small ($\lesssim$1 nm) but clearly evident red-shift for both the cytochrome *b* and a_3 bands of the photolyzed enzyme compared with the equilibrium enzyme. It is interesting that the spectral perturbation of cytochrome *b*, which does not bind exogenous ligands, is comparable to that experienced by cytochrome a_3, the site of ligand binding. Comparable perturbation of heme a_3 and *b* spectra by CO binding at heme a_3 suggests that mechanical forces carried by the protein matrix strongly couple the two heme centers. Direct heme–heme interaction is not shown because the perturbation persists after photodissociation of the CO bond, when the electronic structure of heme a_3 has largely relaxed to its non-CO-ligated state. Rather, protein conformation around heme *b* is perturbed by CO binding at heme a_3 in a manner that is very slow to relax after the heme a_3–CO bond is broken.

The largest spectral shift between photolysis and static difference spectra occurs in the α band region near 613–623 nm (Figure 8). The roughly 10-nm red-shift of the cytochrome a_3 transient is similar to the 15-nm red-shift seen in mammalian cytochrome oxidase (Stoutland et al., 1991). These authors suggest that the a_3 spectral shift may result from structural changes at the cytochrome a_3 center caused by binding of CO to nearby Cu_B. The ca. 1-μs decay of this shift seems to parallel thermal dissociation of the Cu_B–CO bond in cytochrome aa_3.[2] Cu_B–CO perturbation of the cytochrome a_3 center may be associated with the CO-liganded conformation of the protein persisting after photodissociation of cytochrome ba_3. This possibility is consistent with the time scales for spectral relaxation and Cu_B–CO dissociation in the bacterial enzyme, which are both comparable to the Fe–CO recombination time.

Small spectral shifts (1–2 nm) have also been observed between the visible region MCD spectra of equilibrium reduced cytochrome aa_3 and photolyzed enzyme trapped after photodissociation of the CO complex at low temperature (15 K) (Sharanov et al., 1982). The visible MCD of reduced cytochrome aa_3 is strongly temperature dependent because of the presence of *C* terms from paramagnetic cytochrome a_3^{2+} (Thomson et al., 1976). At 293 K, the *C* terms are much smaller than the (temperature-independent) MCD contribution of diamagnetic cytochrome a^{2+}, the latter having a double-lobed shape with positive lobe at longer wavelengths and zero-crossing near 600 nm. At 15 K, on the other hand, the *C* terms from cytochrome a_3 are several times more intense than the MCD contribution of a^{2+} and give an MCD profile that is roughly the mirror image of the high-temperature spectrum, i.e., negative lobe at longer wavelengths. Therefore, the red-shift observed at low temperature mainly reflects a perturbation of heme a_3 electronic energies. In analogy to hemoglobin (Perutz et al., 1974), this perturbation is presumably due to a constraint of the axial coordination geometry of heme a_3 with the proximal histidine. Frozen in a CO-ligated conformation, the protein prevents the Fe–imidazole bond from relaxing to its equilibrium non-CO-ligated geometry. A similar red-shift is observed in the TRMCD spectrum of photolyzed cytochrome aa_3 measured at 100 ns and 10 μs after ambient temperature photodissociation of the CO complex (Goldbeck et al., 1991). However, because the MCD of cytochrome *a* is considerably more intense at ambient temperature than the *C* terms of cytochrome a_3, the persistence of a red-shift at high temperatures suggests a perturbation of cytochrome *a* energies by an unrelaxed, Fe–CO-ligated form of the protein. In any event, the interpretation of spectral shifts, which in this case are quite small compared with spectral bandwidths, is complicated in cytochrome aa_3 by the possibility that ligation changes at cytochrome a_3 or Cu_B associated with ligand shuttle events after CO photodissociation also could affect heme a_3 electronic energies (Goldbeck et al., 1991).

The *A* term contributed by cytochrome b^{2+} to the visible band MCD of reduced cytochrome ba_3 in Figure 3 has a narrow bandwidth (250-cm^{-1} peak to trough splitting). The sharpness of this spectral feature makes the small, 0.4-nm (12-cm^{-1}), red-shift of the band in the photolyzed enzyme, compared with the equilibrium reduced enzyme, evident in Figure 3. This red-shift also appears in the spectrum of the CO complex. Although direct heme–heme interaction could perturb the heme *b* component in the MCD spectrum of the complex, the persistence of heme *b* perturbation after photodissociation of the CO bond indicates here, as in the absorption spectrum of the photolyzed enzyme, that the protein conformation around heme *b* is slow to relax.

The slightly larger peak to trough intensity and small blue-shift (0.4 nm) of the Q_0 MCD band of unliganded cytochrome ba_3 compared with the CO-complexed and photolyzed enzyme may reflect small differences in the geometry of axial coordination of heme B in complexed and unliganded enzyme that persist for at least tens of microseconds after photolysis. A lowering of symmetry in the geometry of axial bonding of the histidine residues to heme B, presumably induced by a global conformational change in the protein as it accommodates heme A–CO bond formation, would tend to lift the degeneracy of the ferrocytochrome *b* Q_0 bands and lower the intensity of the *A* term. Such a protein conformational change could be relatively slow to propagate through the protein and affect the spectrum of heme B after CO photolysis from heme A.

Nature of the Non-Fe_{a_3}–CO Ligated Component. The Soret MCD of the CO–enzyme preparation (Figure 2) contains a peak at 446 nm indicating the sample contains ~30% of a non-CO-ligated, high-spin cytochrome a_3^{2+}. This is surprising given the large CO affinity constants ($\sim 10^6$) typical of oxidases, which should assure saturation under the conditions of our experiment. Previous Mössbauer studies showed that ~86% of reduced, high-spin a_3 is converted to a low-spin form upon exposure to 1 atm of CO and subsequent cooling to 77 K (Zimmermann et al., 1988). If the protein is somehow denatured so as to preclude CO binding to some of the a_3 in the sample, the presence of heterogeneity should lead to broadening of the MCD signal. This is not observed; the line width of the two MCD signals are identical. Therefore, there is no reason to believe that ~30% of a_3 is physically unable to bind CO. We propose that the equilibrium reaction of reduced ba_3 with CO can be written as

$$b^{2+}a_3{}^{2+}{}_{hs},Cu_B + CO_{(aq)} \rightleftharpoons \{b^{2+}a_3{}^{2+}{}_{hs},OC\text{–}Cu_B \rightleftharpoons b^{2+}a_3{}^{2+}{}_{ls}\text{–}CO,Cu_B\}$$

indicating that only one CO can bind at the a_3–Cu_B site, at either the Fe or the Cu. The reaction in brackets shows a thermal equilibrium in which CO is transferred between the two metals of the a_3–Cu_B site. When bound to Fe, the heme A will be low-spin and have a very weak Soret MCD signal. When bound to Cu, the Fe will be high-spin and will have a strong Soret MCD signature. In the photolyzed enzyme, in which the CO is known to be bound to Cu_B (Einarsdóttir et

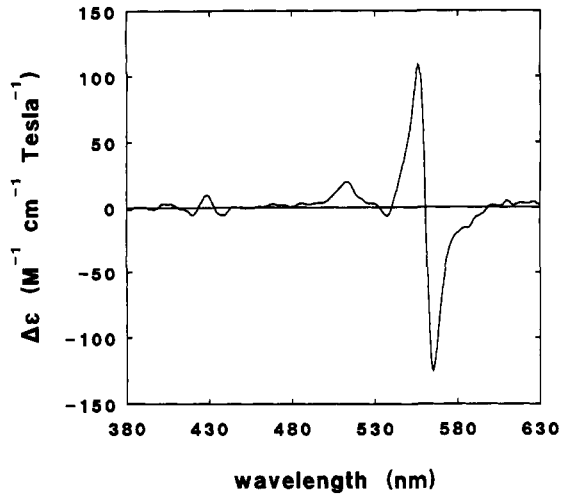

FIGURE 10: MCD spectrum of cytochrome ba_3–CO corrected for full complex formation (f = 1, see eq 10). Because of the MCD silence of low-spin cytochrome a_3–CO, the Soret MCD spectrum of the complex is a good approximation to the spectrum of cytochrome b^{2+} ($b^{\dagger}$ in text).

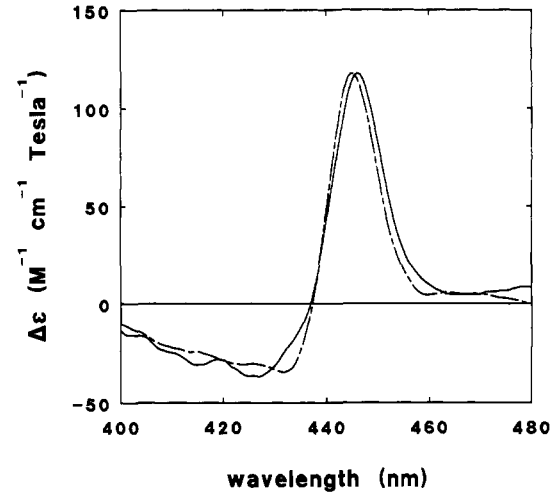

FIGURE 11: Soret region MCD spectrum of photolyzed cytochrome a_3^{2+} ($a_3^{\dagger}$) (—) calculated from eq 13 has a peak at 446 nm. The MCD of equilibrium reduced cytochrome a_3^{2+} (- - -) is blue-shifted by ~1 nm to 445 nm.

al., 1989), the MCD peak is at 446 nm. This peak is red-shifted from that of the equilibrium reduced enzyme by 1 nm, suggesting that the presence of CO on Cu_B affects the MCD spectrum of nearby cytochrome a_3. The non-Fe_{a_3} ligated fraction of the CO preparation has an MCD peak at the same wavelength as the photolyzed enzyme, consistent with the idea that bound CO is thermally distributed between the two metals. As noted above, Mössbauer studies show that there is more nearly quantitative formation of low-spin cytochrome a_3 upon binding CO. The apparent discrepancy between the ambient temperature MCD results and the low-temperature Mössbauer results is probably due to shifting of the equilibrium in brackets toward the right on cooling to cryogenic temperatures.

MCD Difference Spectra. The near UV–vis MCD spectra of reduced cytochrome ba_3, CO complex, and the photolyzed enzyme are composites of individual cytochrome b and a_3 contributions:

$$U = b + a_3$$

$$C = b^{\dagger} + a_3\text{–CO}$$

$$U^* = b^* + a_3^* \qquad (13)$$

The MCD silence of cytochrome a_3-CO allows determination of a_3^* and $b^{\dagger}$ from C and U* using eq 13 and assuming that $a_3,b^{\dagger} \approx a_3,b^*$. Babcock et al. (1976) found that the Soret MCD spectrum of mammalian cytochrome aa_3–CO contains very little contribution from low-spin cytochrome a_3 and that it thus provides a good estimate of the spectrum of individual ferrocytochrome a. Subtraction of this spectrum from the MCD spectrum of the reduced mammalian enzyme yields the spectrum of individual, high-spin cytochrome a_3^{2+}. The MCD spectrum of cytochrome ba_3–CO shows that the Soret MCD intensity of cytochrome a_3–CO is also negligible in the bacterial enzyme, i.e.,

$$C \approx b^{\dagger} \qquad (14)$$

The MCD spectrum of the complex, corrected using eq 10 (f = 0.7, ϕ = 0.8), is shown in Figure 10. It appears to be a typical ferrous b-type cytochrome spectrum, with a positive peak close to the cytochrome b^{2+} absorption peak at 427 nm. It is very similar to the spectra of cytochrome b^{2+} from yeast complex III (T'sai & Palmer, 1982) and cytochrome b_5^{2+} (Vickery et al., 1975; Dolinger et al., 1974).

The individual contribution of high-spin cytochrome a_3^{2+} to the Soret region MCD spectrum of the photolyzed enzyme is estimated by subtracting the cytochrome b^{2+} contribution from the full spectrum of the photolyzed enzyme, i.e., by subtracting eq 10 from eq 9:

$$a_3^* \approx a_3^{\dagger} = U^{\dagger} - C = (OP - OC)/(f\phi) \qquad (15)$$

The MCD spectrum of the cytochrome a_3^* moiety of cytochrome ba_3^* calculated with eq 15 is shown in Figure 11. The Soret bandshape and maximum (446 nm) is very similar to that previously obtained for mammalian cytochrome a_3 by subtracting the spectrum of the cytochrome aa_3–CO complex from the spectrum of reduced cytochrome aa_3 (Babcock et al., 1976). The MCD spectrum of equilibrium cytochrome a_3 is approximated by the spectrum of reduced enzyme, also shown in Figure 11.[3] The equilibrium peak at 445 nm is blue-shifted from the photolyzed a_3 peak by about 1 nm.

Soret MCD and Absorption Spectra of Individual Components. The MCD spectral contributions of individual components of cytochrome ba_3 identified in the present study are summarized in Table III and compared with cytochromes from mammalian oxidase and cytochrome b_5. Most striking are the nearly identical MCD spectra obtained for cytochrome a_3^{2+} from the bacterial and mammalian oxidases. The similarity of a_3 MCD in ba_3 and aa_3 reflects a close similarity in protein environments around the heme a_3 prosthetic groups in the bacterial and mammalian enzymes. Although a very weak Faraday A term centered near 430 nm is assigned to low-spin cytochrome a_3 in mammalian cytochrome aa_3–CO (Babcock et al., 1976), a corresponding band is not observed in cytochrome ba_3–CO, possibly because of overlap by the stronger signal from cytochrome b^{2+}.

The variation of the bacterial a_3–CO absorption band from its mammalian counterpart is evident in the smaller absorption diference spectrum between unliganded and CO-liganded enzyme for ba_3 compared with aa_3, a discrepancy too large

[3] The spectrum of the reduced enzyme contains a component near 429 nm, due to cytochrome b^{2+}, which is probably a ca. 1-nm blue-shifted version of the $b^{\dagger}$ spectrum shown in Figure 10. This accounts for the small difference in blue-edge bandshapes evident in Figure 11.

Table III: Soret Region MCD Spectral Characteristics of Individual Cytochrome Components

species	spin state	MCD origin	band extrema (nm)	$\Delta\epsilon/H$ (M^{-1} cm^{-1} $tesla^{-1}$)
ferric				
b^{3+}	low	*C*	405	42
		C	421	−63
b_5^{3+} [b]	low	*C*	407	73
		C	419	−97
a^{3+} [a]	low	*C*	420	20
		C	434	−40
a_3^{3+}	high	inactive		
ferrous				
b^{2+}	low	*A,B*	429	10
b_5^{2+} [b]	low	*A,B*	426	20
a^{2+} [a]	low	*A*	452	56
		A	438	−50
a_3^{2+} [c]	high	*C*	427	−37
		C	446	118
a_3^{2+} [a]	high	*C*	429	−26
		C	445	96
a_3^{2+}–CO	low	*A*	429	4
		A	435	−4
a_3^{2+}–CO[a]	low	*A*	423	5
		A	434 (shoulder)	

[a] Bovine heart cytochrome aa_3: band extrema and $\Delta\epsilon/H$ from Goldbeck et al. (1991); Faraday *A* and *C* assignments from Babcock et al. (1976). [b] Porcine liver cytochrome b_5, from Vickery et al. (1976). [c] Photolyzed enzyme (a_3*).

to be accounted for by incomplete complex formation alone. The component absorption spectra of cytochrome aa_3 have been deconvoluted by Vanneste (1966). This analysis starts by using the photochemical action spectrum of the CO complex (Nicholls & Chance, 1974) to provide an absorption spectrum for individual cytochrome a_3–CO. The Soret band of the latter is centered near 430 nm in aa_3. The Soret absorption band maxima of a_3^{2+} and a^{2+} are at 442 and 444 nm, respectively. While the absorption data presented here is insufficient to support a similar ab initio deconvolution of spectral components for ba_3, a spectrum can be determined for a_3–CO from the corrected spectrum of the complex if certain assumptions are made about other spectral parameters. With the following assumptions, (1) the absorption spectrum of bacterial a_3^{2+} is identical to the mammalian spectrum and (2) the cytochrome b^{2+} band center is at 427 nm, the a_3–CO band is found to be centered at 433 nm with a half width at half maximum of 8 nm.

Fe–CO Binding. Three lines of evidence indicate that binding of CO to Fe_{a_3} is weaker in cytochrome ba_3 than in cytochrome aa_3: (1) the smaller unliganded *minus* CO complex difference absorption spectrum, (2) the incomplete formation of CO complex, and (3) the unusually high IR stretching frequencies of heme-bound CO in cytochrome ba_3. In cytochrome aa_3, the Soret band of cytochrome a_3 shifts from 442 nm in the reduced enzyme to ca. 430 nm in the CO complex, a red-shift of roughly 12 nm with binding of CO to Fe. The cytochrome a_3–CO band center appears to be shifted to the red by several nanometers in cytochrome ba_3 from the a_3–CO band center in cytochrome aa_3. A concomitant line broadening also reduces the size of the photolysis difference spectrum and contributes to its asymmetric shape. The net result of both effects is a red-shift of the trough corresponding to cytochrome a_3–CO bleaching from 427 nm in aa_3 to 430 nm in ba_3 along with reduced intensity compared with the peak. The spectral broadening indicates a greater heterogeneity of Fe–CO interactions in ba_3, consistent with the evidence for multiple Fe–CO conformers in the IR spectrum (Einarsdóttir et al., 1989). If the size of the reduced *minus* Fe–CO complex difference spectrum is taken as an indicator of the strength of Fe–CO interaction, then this interaction is diminished by 30% in ba_3 from aa_3. Formation of cytochrome aa_3–CO goes essentially to completion under typical conditions (10^{-5} M enzyme, 1 atm CO), whereas 30% of cytochrome ba_3 remains non-Fe–CO liganded. Under the likely assumption that most of the non-Fe–CO ligated ba_3 is in the Cu_B–CO form, the relevant equilibrium is

$$Fe_{a_3},Cu_B\text{–}CO \rightleftharpoons Fe_{a_3}\text{–}CO,Cu_B$$

The observed ratio of CO-liganded Fe to non-CO-liganded Fe corresponds to an equilibrium constant of 2.3, or ΔG° = −0.5 kcal/mol. The presence of this equilibrium suggests that the Fe_{a_3}–CO bond is less thermodynamically stable in cytochrome ba_3 than in cytochrome aa_3, allowing the adjacent Cu_B to effectively compete for coordination to CO. Additional evidence for weakened Fe–CO interaction comes from IR frequencies measured for CO in oxidase complexes. The ν_{CO} of CO bound to Fe is blue-shifted by about 16 cm^{-1} from the major peak observed in cytochrome aa_3 at 1963 cm^{-1} (Einarsdóttir et al., 1989).[4] Indeed, cytochrome ba_3–CO has the highest heme-bound CO frequency reported for a heme protein–CO complex. The CO peaks of both oxidases are blue-shifted compared with ν_{CO} observed in hemoglobin and myoglobin complexes, 1940–1950 cm^{-1} (Shimada & Caughey, 1982; Choc & Caughey, 1982). The blue-shift of ν_{CO} toward the value for free CO (2140 cm^{-1}) shows a weakening of the Fe–CO interaction. In contrast, ν_{CO} for CO bound to Cu_B is quite similar in ba_3 (2053 cm^{-1}) and aa_3 (three bands centered near 2053 cm^{-1}), suggesting that the Cu–CO bond strengths are similar in the two proteins.

CD of Heme Chromophores. Since hemes A and B do not have intrinsic CD, the Soret and visible CD bands are probably induced by interactions with asymmetrically arrayed aromatic residues near the hemes, as in myoglobin and hemoglobin (Hsu & Woody, 1971). The Soret CD spectra of oxidized, reduced, and CO-complexed cytochrome ba_3 share a bisignate, double-lobed shape with positive lobe at lower energy. There are several ways such a bandshape can arise in cytochrome ba_3. Excitonic heme–heme interactions may cause bisignate bandshape, but the absence of excitonic CD in the spectrum of reduced cytochrome aa_3 (Myer, 1985) and the lack of evidence for electronic heme–heme interaction in the MCD of cytochrome ba_3 argues against this explanation. Hsu and Woody (1971) have shown that CD induced in the Soret bands of a single heme chromophore by interactions with aromatic residues can acquire a bisignate band shape from splitting of the Soret degeneracy. The sign of the resulting bandshape depends on the polarization orientation of the heme transitions compared with the protein matrix. This mechanism may account for the bisignate CD deduced by Myer (1985) for cytochrome a_3–CO in mammalian oxidase. Bisignate bandshape also can arise in cytochrome ba_3 from inequivalent hemes having oppositely signed CD. The absolute CD spectra of cytochromes a^{2+} and a_3^{2+} have been deconvoluted from the CD spectrum of mammalian cytochrome oxidase as positive, near-Gaussian bands centered at 444 and 445 nm, respectively.[5] The positive CD lobe in reduced bacterial enzyme appears to be largely associated with cytochrome a_3 because of the spectral overlap with mammalian a_3, blue-shift with

[4] Overlapping bands at 1974 and 1983 cm^{-1} correspond to CO stretching frequencies for two of multiple heme a_3–CO conformers present in cytochrome ba_3.

[5] Hemoglobin and myoglobin have similar positive band CD in the Soret region (Myer & Pande, 1978).

CO binding and red-shift in the photolyzed enzyme. The negative band at higher energy is closer to the absorption maximum of cytochrome *b* and shifts very little with CO binding. The assignment of this CD band to cytochrome b^{2+} is consistent with the observation that *b*-type cytochromes often possess an intense negative CD band centered close to the Soret absorption maximum (Okada & Okunuki, 1970). The increase in negative ellipticity near 420 nm that accompanies CO binding is assigned to the bisignate ellipticity induced in cytochrome a_3 that is observed in cytochrome aa_3–CO.

CONCLUSIONS

The MCD and CD spectra of the steady-state forms of *Thermus* cytochrome ba_3 reported here support previous assignments of heme center valence and spin configurations (Zimmerman et al., 1988). The heme A and B spin state assignments discussed here for the MCD spectra are also seen in the Mössbauer spectra of the reduced enzyme and its CO complex (Zimmerman et al., 1988). In the oxidized enzyme, cytochrome *b* is low-spin ferric whereas cytochrome a_3 is high-spin ferric; in the reduced enzyme, cytochrome *b* is low-spin ferrous whereas cytochrome a_3 is high-spin ferrous; and in the CO liganded enzyme, both cytochrome *b* and a_3 are low-spin ferrous. As in the aa_3 type oxidases, cytochrome a_3 is the binding site for exogenous ligands, such as CO and O_2. Our data suggest that, in cytochrome ba_3, CO thermally distributes between coordination to cytochrome a_3 and Cu_B.

The TRMCD results for ba_3 show that $Fe_{a_3}{}^{2+}$ goes to a high-spin configuration upon CO photodissociation and remains in this spin configuration until CO recombines with the iron, as observed previously in cytochrome aa_3. The appearance of unliganded Fe is probably a subpicosecond event since Fe–CO bond breaking and electronic relaxation of the photolyzed heme appears to be complete within roughly 100 fs in cytochrome aa_3 (Stoutland et al., 1991) and hemoglobin (Martin et al., 1983). The photoinitiated transfer of CO from Fe_{a_3} to Cu_B is known to occur in less than 1 ps in cytochrome aa_3–CO, making it the fastest observed ligation reaction (Dyer et al., 1991). The much longer time scale ($\gg$10 μs) for relaxation of the energies of the MCD and CD band extrema of cytochrome $a_3{}^{2+}$ in cytochrome ba_3 to those characteristic of the unliganded enzyme shows that the protein environment around a_3 adjusts very slowly to ligand loss.

The high-spin $Fe_{a_3}{}^{2+}$ state achieved after photodissociation of CO is spectrally distinct from that observed in steady-state, reduced-enzyme; moreover, the spectral characteristics of the equilibrium enzyme are not recovered at room temperature before recombination with CO occurs milliseconds after photolysis. Similarly, photolysis of the CO-liganded form induces small changes in the spectral features of $Fe_b{}^{2+}$ (most evident in the visible MCD spectra of Figure 3); these differences also persist until recombination with CO occurs. Photolysis thus appears to leave the reduced cytochrome ba_3 molecule in a metastable state in which both heme centers possess slightly different structural environments when compared with the steady-state, unliganded enzyme. The simplest interpretation of these results is that the reduced enzyme undergoes a small but "global" structural change upon ligation by CO that is not reversed during a time period of tens of microseconds after photolysis at room temperature, although more complicated interpretations are possible (Woodruff et al., 1991). The persistence of ligated protein structure after Fe–CO photodissociation may be caused by a high activation barrier for protein relaxation or may be associated with concomitant Cu_B–CO binding. The spectral differences between photolyzed cytochrome ba_3 and equilibrium unliganded enzyme persist on a time scale comparable to the events of ligand rebinding. This finding for cytochrome ba_3 emphasizes the importance of considering possible structural differences between equilibrium and photolyzed oxidases in the interpretation of flow-flash O_2 binding studies that employ photolyzed enzyme as a surrogate for physiologically reduced, unliganded enzyme.

REFERENCES

Anraku, Y. (1988) *Annu. Rev. Biochem. 57*, 101–132.

Babcock, G. T., Vickery, L. E., & Palmer, G. (1976) *J. Biol. Chem. 251*, 7907–7919.

Babcock, G. T., Jean, J. M., Johnston, L. N., Palmer, G., & Woodruff, W. H. (1984) *J. Am. Chem. Soc. 106*, 8305–8306.

Blackmore, R. S., Greenwood, C., & Gibson, Q. H. (1991) *J. Biol. Chem. 266*, 19245–19249.

Capaldi, R. A. (1990) *Annu. Rev. Biochem. 59*, 569–596.

Carter, K., & Palmer, G. (1982) *J. Biol. Chem. 257*, 13507–13514.

Chan, S. I., & Li, P. M. (1990) *Biochemistry 29*, 1–12.

Chance, B., Saronio, C., & Leigh, J. S., Jr. (1975) *Proc. Natl. Acad. Sci. U.S.A. 72*, 1635–1640.

Chepuri, V., Lemieux, L., Au, D. C. T., & Gennis, R. B. (1990) *J. Biol. Chem. 265*, 11185–11192.

Choc, M. G., & Caughey, W. S. (1982) *J. Biol. Chem. 256*, 1831–1838.

Dawes, T. D. (1990) Ph.D. dissertation, University of California at Santa Cruz.

Dawson, J. H., & Dooley, D. M. (1989) in *Iron Porphyrins, Part III; Physical Bioinorganic Chemistry Series* (Lever, A. B. P., & Gray, H. B., Eds.) Vol. 4, pp 1–136, VCH, New York.

Djerassi, C., Lu, Y., Waleh, A., Shu, A. Y. L., Goldbeck, R. A., Kehres, L. A., Crandell, C. W., Wee, A. G. H., Knierzinger, A., Gaete-Holmes, R., Loew, G., Clezy, P. S., & Bunnenberg, E. (1984) *J. Am. Chem. Soc. 106*, 4241–4258.

Dolinger, P. M., Kielczewski, M., Trudell, J. R., Barth, G., Linder, R. E., Bunnenberg, E., & Djerassi, C. (1974) *Proc. Natl. Acad. Sci. U.S.A. 71*, 399–403.

Dyer, R. B., Einarsdóttir, Ó., Killough, P. M., López-Garriga, J. J., & Woodruff, W. H. (1989) *J. Am. Chem. Soc. 111*, 7657–7659.

Dyer, R. B., Peterson, K. A., Stoutland, P. O., & Woodruff, W. H. (1991) *J. Am. Chem. Soc. 113*, 6276–6277.

Einarsdóttir, Ó., & Caughey, W. S. (1985) *Biochem. Biophys. Res. Commun. 129*, 840–847.

Einarsdóttir, Ó., Killough, P. M., Fee, J. A., & Woodruff, W. H. (1989) *J. Biol. Chem. 264*, 2405–2408.

Fee, J. A., Kuila, D., Mather, M. W., & Yoshida, T. (1986) *Biochim. Biophys. Acta 853*, 153–185.

Fee, J. A., Mather, M. W., Springer, P., Hensel, S., & Buse, G. (1988) *Ann. N.Y. Acad. Sci. 550*, 33–38.

Fiamingo, F. G., Altschuld, R. A., Moh, P. P., & Alben, J. O. (1982) *J. Biol. Chem. 257*, 1639–1650.

Goldbeck, R. A. (1988) *Acc. Chem. Res. 21*, 95–101.

Goldbeck, R. A., Dawes, T. D., Milder, S. J., Lewis, J. W., & Kliger, D. S. (1989) *Chem. Phys. Lett. 156*, 545–549.

Goldbeck, R. A., Dawes, T. D., Einarsdóttir, Ó., Woodruff, W. H., & Kliger, D. S. (1991) *Biophys. J. 60*, 125–134.

Hsu, M.-C., & Woody, R. W. (1971) *J. Am. Chem. Soc. 93*, 3515–3525.

Kliger, D. S., Lewis, J. W., & Goldbeck, R. A. (1989) *Proc. SPIE Int. Soc. Opt. Eng. 1057*, 26–33.

Kliger, D. S., Lewis, J. W., & Randall, C. E. (1990) *Polarized Light in Optics and Spectroscopy*, pp 176–178, Academic, Boston.

Martin, J.-L., Migus, A., Poyart, C., Lecarpentier, Y., Astier, R., & Antonetti, A. (1983) *Proc. Natl. Acad. Sci. U.S.A. 80*, 173–178.

Mather, M. W., Springer, P., & Fee, J. A. (1990) in *Proceedings of the 41st Mosbach Colliquium* (Hauska, G., & Thauer, R., Eds.) pp 94–104, Springer Verlag, New York.
Mather, M. W., Springer, P., & Fee, J. A. (1991) *J. Biol. Chem. 266*, 5025–5035.
Michl, J. (1978) *J. Am. Chem. Soc. 100*, 6801–6811, 6812–6818.
Myer, Y. P. (1985) *Curr. Top. Bioenerg. 14*, 149–188.
Myer, Y. P., & Pande, A. (1978) in *The Porphyrins* (Dolphin, D., Ed.) Vol. 3, pp 271–322, Academic Press, New York.
Nicholls, P., & Chance, B. (1974) in *Molecular Mechanisms of Oxygen Activation* (Hayaishi, O., Ed.) pp 479–534, Academic Press, New York.
Okada, Y., & Okunuki, K. (1970) *J. Biochem. (Tokyo) 67*, 487–496.
Pan, L. P., Li, Z., Larsen, R., & Chan, S. I. (1991) *J. Biol. Chem. 266*, 1367–1370.
Perutz, M. F., Heidner, E. J., Ladner, J. E., Beetlestone, J. G., Ho, C., & Slade, E. F. (1974) *Biochemistry 13*, 2187–2200.
Puustinen, I., & Wikström, M. (1991) *Proc. Natl. Acad. Sci. U.S.A. 88*, 6122–6126.
Saraste, M. (1990) *Q. Rev. Biophys. 23*, 331–366.
Savitzky, A., & Golay, M. J. E. (1964) *Anal. Chem. 36*, 1627–1639.
Scott, R. A. (1989) *Annu. Rev. Biophys. Biophys. Chem. 18*, 137–158.
Sharanov, Y. A., Sharanova, N. A., Figlovsky, V. A., & Grigorjev, V. A. (1982) *Biochim. Biophys. Acta 709*, 332–341.
Shimada, H., & Caughey, W. S. (1982) *J. Biol. Chem. 257*, 11893–11900.
Stoutland, P. O., Lambry, J.-C., Martin, J.-L., & Woodruff, W. H. (1991) *J. Phys. Chem. 95*, 6406–6408.
Thomson, A. J., Brittain, T., Greenwood, C., & Springall, J. (1976) *FEBS Lett. 67*, 94–98.
T'sai, A.-H., & Palmer, G. (1982) *Biochim. Biophys. Acta 681*, 484–495.
Vanneste, W. H. (1966) *Biochemistry 5*, 838–848.
Vickery, L., Salmon, A., & Sauer, K. (1975) *Biochim. Biophys. Acta 386*, 87–98.
Vickery, L., Nozawa, T., & Sauer, K. (1976) *J. Am. Chem. Soc. 98*, 351–357.
Wikström, M., Krab, K., & Saraste, M. (1981) *Cytochrome Oxidase: A Synthesis*, Academic Press, New York.
Wikström, M., Saraste, M., & Penttilä, T. (1985) in *The Enzymes of Biological Membranes, Vol. 4, Bioenergetics of Electron and Proton Transport* (Martonosi, A. N., Ed.) pp 111–148, Plenum, New York.
Woodruff, W. H., Einarsdóttir, Ó., Dyer, R. B., Bagley, K. A., Palmer, G., Atherton, S. J., Goldbeck, R. A., Dawes, T. D., & Kliger, D. S. (1991) *Proc. Natl. Acad. Sci. U.S.A. 88*, 2588–2592.
Yoshida, T., Lorence, R. M., Choc, M. G., Tarr, G. E., Findling, K. L., & Fee, J. A. (1984) *J. Biol. Chem. 259*, 112–123.
Zimmerman, B. H. (1989) Ph.D. dissertation, Louisiana State University.
Zimmerman, B. H., Nitsche, C. I., Fee, J. A., Rusnak, R., & Münck, E. (1988) *Proc. Natl. Acad. Sci. U.S.A. 85*, 5779–5783.

Registry No. CO, 630-08-0; cytochrome ba_3, 9035-37-4; cytochrome a_e, 72841-18-0.